Earth's Future

RESEARCH ARTICLE
10.1029/2022EF003268

Projected Impact of Increased Global Warming on Heat Stress and Exposed Population Over Africa

Thierry C. Fotso-Nguemo[1,2,3], Torsten Weber[1], Arona Diedhiou[3,4], Steven Chouto[2,5], Derbetini A. Vondou[6], Diana Rechid[1], and Daniela Jacob[1]

[1]Climate Service Center Germany (GERICS), Helmholtz-Zentrum Hereon, Hamburg, Germany, [2]Climate Change Research Laboratory (CCRL), National Institute of Cartography, Yaounde, Cameroon, [3]Laboratoire Mixte International "Nexus Climat-Eau-Énergie-Agriculture en Afrique de l'Ouest et Services Climatiques" (LMI NEXUS), Université Félix Houphouët-Boigny, Abidjan, Côte d'Ivoire, [4]University of Grenoble Alpes, IRD, CNRS, Grenoble INP, IGE, Grenoble, France, [5]Department of Geography, Higher Teacher Training College, University of Maroua, Maroua, Cameroon, [6]Laboratory for Environmental Modelling and Atmospheric Physics (LEMAP), Department of Physics, Faculty of Science, University of Yaounde 1, Yaounde, Cameroon

Abstract This study investigates the impact of increased global warming on heat stress changes and the potential number of people exposed to heat risks over Africa. For this purpose a heat index has been computed based on an ensemble-mean of high-resolution regional climate model simulations from the Coordinated Output for Regional Evaluations embedded in the COordinated Regional Climate Downscaling EXperiment, under two Representative Concentration Pathways (RCPs) scenarios (RCP2.6 and RCP8.5), combined with projections of population growth developed based on the Shared Socioeconomic Pathways (SSPs) scenarios (SSP1 and SSP5). Results show that by the late 21st century, the increased global warming is expected to induce a 12-fold increase in the area extent affected by heat stress of high-risk level. This would result in an increase of about 10%–30% in the number of days with high-risk heat conditions, as well as about 6%–20% in their magnitude throughout the seasonal cycle over West, Central, and North-East Africa. Therefore, and because of the lack of adaptation and mitigation policies, the exacerbation of ambient heat conditions could contribute to the exposure of about 2–8.5 million person-events to heat stress of high-risk level over Burkina Faso, Ghana, Niger, and Nigeria. Furthermore, it was found that the interaction effect between the climate change and population growth seems to be the most dominant in explaining the total changes in exposure due to moderate and high heat-related risks over all subregions of the African continent.

Plain Language Summary This study investigates the impact of increased global warming on heat stress changes and the potential number of persons likely to be exposed to heat risks over Africa. Results show that by the end of the 21st century, the increased global warming is expected to induce a 12-fold increase in the total area affected by dangerous heat conditions over the continent. This would result in an increase of about 10%–30% in the number of days with these heat conditions, as well as about 6%–20% in their magnitude throughout the seasonal cycle over West, Central and North-East Africa. Therefore, because of the lack of adaptation and mitigation policies, the exacerbation of ambient heat conditions could contribute to the exposure of about 2–8.5 million person-events to heat stress of high-risk level over Burkina Faso, Ghana, Niger, and Nigeria. Since these heat events would be partly driven by interactions effects between climate change and population growth, efficient measures allowing not only to mitigate the increased greenhouse gas emissions, but also the effects of high heat on the human body must be urgently implemented on the affected countries' scale, in order to significantly decrease the vulnerability of their populations to potential heat-related health problems.

Key Points:

- Increased global warming induces more spatially and temporally widespread extreme heat events over West, Central and North-East Africa
- Populations of some West African countries are projected to be particularly exposed to moderate and high heat conditions
- Change in population exposure to dangerous heat categories is mainly driven by the interaction effect between climate and population growth

Supporting Information:

Supporting Information may be found in the online version of this article.

Correspondence to:

T. C. Fotso-Nguemo,
thierry.fotso-nguemo@hereon.de;
fotso.nguemo@gmail.com

Citation:

Fotso-Nguemo, T. C., Weber, T., Diedhiou, A., Chouto, S., Vondou, D. A., Rechid, D., & Jacob, D. (2023). Projected impact of increased global warming on heat stress and exposed population over Africa. *Earth's Future*, *11*, e2022EF003268. https://doi.org/10.1029/2022EF003268

Received 13 JUL 2022
Accepted 14 DEC 2022

Author Contributions:

Conceptualization: Thierry C. Fotso-Nguemo, Torsten Weber
Data curation: Thierry C. Fotso-Nguemo, Derbetini A. Vondou
Formal analysis: Thierry C. Fotso-Nguemo
Funding acquisition: Torsten Weber, Arona Diedhiou
Investigation: Thierry C. Fotso-Nguemo

1. Introduction

During the last decades, most of African countries have experienced a trend of warming, which has been increasing at rates higher than the global average rate of temperature increase (Colin, 2011). According to the Intergovernmental Panel on Climate Change's report (IPCC, 2022), climate change risks will rapidly increase in the mid-to-long term with continued global warming, particularly in areas already exposed to high temperatures. Furthermore, projections also suggest that by 2050, half of the net increase in the world's population is expected to be concentrated in Sub-Saharan Africa, leading to high urbanization rates and extensive land cover changes

Methodology: Thierry C. Fotso-Nguemo, Torsten Weber
Resources: Torsten Weber, Diana Rechid, Daniela Jacob
Software: Thierry C. Fotso-Nguemo, Torsten Weber, Derbetini A. Vondou
Supervision: Torsten Weber, Arona Diedhiou
Validation: Thierry C. Fotso-Nguemo, Torsten Weber, Arona Diedhiou, Diana Rechid, Daniela Jacob
Visualization: Thierry C. Fotso-Nguemo, Arona Diedhiou, Steven Chouto, Derbetini A. Vondou, Diana Rechid
Writing – original draft: Thierry C. Fotso-Nguemo
Writing – review & editing: Thierry C. Fotso-Nguemo, Torsten Weber, Arona Diedhiou, Steven Chouto, Derbetini A. Vondou, Diana Rechid, Daniela Jacob

(Forget et al., 2021). Given the ambient climatic threat, coupled with the high demographic growth as well as the low capacity and resilience partly due to endemic poverty of its population, the African continent is particularly vulnerable to climate hazards through exposure to a wide range of climate risks (Opoku et al., 2021). Among these hazards, those related to extreme heat, which in fact result from the combination of natural and human stressors (e.g., high air temperature, high air humidity, high population density, among others), will continue to significantly increase with additional warming, especially without further adaptation efforts (IPCC, 2022). This would contribute to a substantial worsening of the potential impacts that these extreme events can have on the socio-economic development of nations (IPCC, 2022; Parkes et al., 2019), and therefore will represent one of the main challenges for decision makers of the continent.

It is commonly known that the level of discomfort experienced in warm weather environment, is directly linked to the amount of incident solar radiation as well as the evaporation rate of the considered region (Diffenbaugh et al., 2007; Pal & Eltahir, 2016). This discomfort which is in fact a consequence of heat stress occurs when the human body is exposed to high temperatures and high humidity for a certain time (Lucas et al., 2014). Despite some internal acclimatization processes which vary according to the metabolism of each individual, human body has an absolute limit of tolerance to heat stress exposure (Medina-Ramon & Schwartz, 2007). Beyond that limit, severe repercussions can be recorded, particularly on health through heat cramps, heat exhaustion and heat stroke, and sometimes even premature death (Rothfusz, 1990; Scovronick et al., 2018). Epidemiological research on temperature mortality functions has shown that elderly people and children are the most vulnerable to these heat-related health risks (Burkart et al., 2014). In addition to age, factors such as gender, ethnicity, pre-existing health problems, education, income level and population density can also increase vulnerability to the harmful heat-related health effects (Burkart et al., 2014). Therefore, future health-related risks induced by heat stress would be strongly influenced by socio-demographic changes, including population growth, aging population and urbanization patterns, as well as social vulnerability (Jagarnath et al., 2020).

In the past, the severity of impacts of heat stress events has been largely ignored over the African continent. This is probably the reason for the particular attention they have received in recent years. In this regard, several studies have been conducted to investigate the future impact of heat stress over Africa in response to increasing global warming. For example, the study of Asefi-Najafabady et al. (2018), based on the high-resolution Community Earth System Model simulations and carried out over some countries located over the East African subregion, revealed that the greatest increases in the number of days of occurrence of heat stress days is likely to occur in the future over the northern and western parts of Kenya, Uganda, and Democratic Republic of Congo (DRC). These authors also concluded that this projected increase in the number of hot days would induce an exposure of local populations to extreme heat stress up to 269-fold higher, strongly driven by demographic and urbanization dynamics. The results of Yengoh and Ardö (2020) over the same subregion are consistent with these trends, indicating that the periods of February–March and August–September are those where high heat intensities are likely to occur in the 2050 and 2100 horizons. Although the issue of heat stress is not the main concern over some cities of South Africa, Jagarnath et al. (2020) showed an increase in their severity, which would impact the most disadvantaged social classes, both in rural and urban locations. Furthermore, in their investigations based on an ensemble-mean of 22 Regional Climate Models (RCMs) simulations over the West African subregion, Sylla et al. (2018) showed a trend toward an increase in the spatial extent as well as the number of days per year of moderate and high hazardous heat stress events. These conditions of high heat felt are likely to severely affect the majority of populations of countries crossed by the Sahelian area of the studied subregion, especially when the global warming level will have reached the threshold of 2°C. Recently in their work based on an ensemble-mean of 8 RCMs, Fotso-Nguemo et al. (2021) found that these high heat-related risks for human health were expected to be 3-fold for thresholds ranging from 1.5°C to 3°C over the northern and central parts of the Central African subregion, with repercussions on the socio-economic development of the affected countries through decreased workers' productivity and increased cooling degree days. In a wider perspective based on an ensemble-mean of five Global Circulation Models (GCMs) simulations, the results of Liu et al. (2017) highlight the fact that out of the increase in the world population's exposure to extreme heat events by the end of the 21st century, Africa alone records a 118-fold increase compared to 4-fold over Europe.

Alongside the above studies, which are focused on extreme heat events, some authors have looked at other extreme weather events combined with population change, which can also have severe consequences on the socio-economic development of the affected countries (e.g., Ayugi et al., 2022; Bouwer, 2013; Weber et al., 2020; among authors). Although these studies have investigated the combination of climate and population change, most

of them focused their attention just on certain subregions or countries of Africa (Asefi-Najafabady et al., 2018; Fotso-Nguemo et al., 2021; Iyakaremye et al., 2021; Jagarnath et al., 2020; Ma & Yuan, 2021; Sylla et al., 2018; Yengoh & Ardö, 2020). Nevertheless, to our knowledge a more comprehensive view of the spatiotemporal variation of heat stress days based on RCMs, as well as the relative importance of the different drivers of change in the projected population exposure to these heat events at continental scale, has not yet been proposed. Such information could be useful for the implementation of efficient adaptation and mitigation strategies, by helping policy makers to better target countries/areas as well as months of the year that are particularly vulnerable to the adverse effects of heat-related hazards. In addition, identifying areas across the continent that are likely to less changes in dangerous heat-related risks, and therefore can serve as a refuge for populations, could also be revealed.

In this context of lack of continental studies that combines heat stress and population changes, this study use the projections of heat index computed based on an ensemble-mean of high-resolution RCMs, performed in the framework of the Coordinated Output for Regional Evaluations (CORE) embedded in the COordinated Regional Climate Downscaling EXperiment (CORDEX; hereafter CORDEX-CORE) initiative (e.g., Ciarlò et al., 2021; Giorgi et al., 2022; Remedio et al., 2019; Teichmann et al., 2021) to explore the response of increased anthropogenic radiative forcing on heat stress changes toward the end of the 21st century in terms of spatial extent, seasonality and number of days of occurrence. Furthermore, the projections of population growth developed based on the new Shared Socioeconomic Pathways (SSPs; Jones & O'Neill, 2016) scenario, will be employed to estimate not only the changes in the potential number of person exposed to these extreme heat events, but also the relative importance of the different drivers of these projected changes. The rest of this document is structured as follows: First, the data sets and methodology used in the work are described in Section 2. Afterward, the results are presented and discussed in Sections 3 and 4, respectively. Conclusion on the main results will follow in Section 5.

2. Data Used and Methodology

2.1. Data

For the analyses of the potential changes in heat stress variations, we considered daily data of mean air temperature (T) as well as relative humidity (RH), from an ensemble-mean of 9 RCMs simulations members, performed in the framework of the CORDEX-CORE project (e.g., Ciarlò et al., 2021; Giorgi et al., 2022; Remedio et al., 2019; Teichmann et al., 2021). In fact, the CORDEX-CORE experiments used in this study have consisted in the use of 3 RCMs named CCLM5, REMO2015, and RegCM4.7, to dynamically downscale 3 same GCMs (HadGEM-ES, MPI-ESM-LR, and NorESM1-M; but the RegCM4.7 has used MPI-ESM-MR) involved in the Phase 5 of the Coupled Model Intercomparison Project (Taylor et al., 2012), at horizontal resolution of about 25 km (~0.22°) instead of about 50 km (~0.44°) as done with the previous CORDEX models (Nikulin et al., 2012).

In this work, all downscaling experiments covering the 1970–2100 period were performed over the CORDEX-Africa domain, by considering two Representative Concentration Pathways (RCPs; Moss et al., 2010) scenarios: (a) a low scenario RCP2.6, which considers some mitigation measures that could control greenhouse gases emissions; and (b) a high scenario RCP8.5, which describes a situation in which radiative forcing reaches 8.5 W/m^{-2} by 2100, without implementing any GHG-emission mitigation policies. Therefore for each RCM member, three 30-year time slice periods were chosen as follows: one historical (1979–2008) representing the baseline period, and two future (2069–2098) representing the projections under the two chosen scenarios. For brevity, details on the nine considered RCMs outputs members, resulting from the dynamical downscaling of different GCMs can be found in Table S1 in Supporting Information S1. It is worth noting that all RCMs used in this study have been already validated in numerous studies conducted over the African continent (e.g., Ciarlò et al., 2021; Diallo et al., 2016, 2018; Dosio et al., 2021; Fotso-Kamga et al., 2020; Fotso-Nguemo et al., 2016, 2019; Giorgi et al., 2022; Nikulin et al., 2012; Pokam et al., 2018; Remedio et al., 2019; Taguela et al., 2020; Tamoffo et al., 2019, 2022; Teichmann et al., 2013, 2021; Vondou & Haensler, 2017; Weber et al., 2018; among others). It was found that the performance of these models varies depending on the considered season and subregion. Moreover, it was shown that the multi-model ensemble-mean performs better than the individual models.

Changes in the population exposure, have been analyzed by considering historical data from the protocol 2b of the Inter-Sectoral Impact Model Intercomparison Project (ISIMIP2b; https://www.isimip.org), as well as projection of the total population data from the NASA Socioeconomic Data and Applications Center (SEDAC; https://sedac.ciesin.columbia.edu). The ISIMIP2b data sets are annual data covering the 1861–2005 period at horizontal resolution of 5 arc-minutes (~0.083°), whereas the SEDAC data sets are decadal data covering the 2010–2100 period at horizontal

Table 1
Heat Index Classification, Along With Their Corresponding Risks Levels, and the Health Problems They Can Trigger

HI (°F)	HI (°C)	Risk levels	Classification	Associated health problems
<80	<27	Extremely low	Safe	No significant stress
[80; 90[	[27; 32[	Low	Caution	Fatigue possible with prolonged exposure and/or physical activity
[90; 105[	[32; 41[	Moderate	Extreme caution	Heat cramps, heat exhaustion, and heat stroke possible with prolonged exposure and/or physical activity
[105; 130[	[41; 54[	High	Danger	Heat cramps and heat exhaustion are likely. Heat stroke probable with prolonged exposure and/or physical activity
≥130	≥54	Very high	Extreme danger	Heat stroke is highly likely and imminent

resolution of 7.5 arc-minutes (~0.125°) and generated according to the new SSPs scenario, which take into account amongst other: (a) the trends in population growth; (b) the educational composition; and (c) the urbanization and gross domestic product (Jones & O'Neill, 2016). Since the estimated ISIMIP2b population data are only available until the end of 2005, the computed average population only includes 27 years for the baseline period. Furthermore, due to the fact that the estimated SEDAC population are given at 10-year intervals, we have computed the average over the years 2070, 2080, 2090, and 2100 from each considered SSPs for the 2069–2098 future period.

2.2. Methodology

The heat stress induced by the combined effects of both high T and RH, has been assessed by considering the heat index (hereafter HI) formulation, based on a multiple regression equation of apparent temperature developed by Steadman (1979) and adapted by the United States National Weather Service (Rothfusz, 1990), as follow:

$$\begin{aligned}\mathbf{HI} = &-\mathbf{42.379} + \mathbf{2.04901523} \times \boldsymbol{T} + \mathbf{10.14333127} \times \mathbf{RH} - \mathbf{0.22475541} \times \boldsymbol{T} \times \mathbf{RH} \\ &- \mathbf{6.83783} \times \mathbf{10}^{-3} \times \boldsymbol{T}^2 - \mathbf{5.481717} \times \mathbf{10}^{-2} \times \mathbf{RH}^2 + \mathbf{1.22874} \times \mathbf{10}^{-3} \times \boldsymbol{T}^2 \times \mathbf{RH} \\ &+ \mathbf{8.5282} \times \mathbf{10}^{-4} \times \boldsymbol{T} \times \mathbf{RH}^2 - \mathbf{1.99} \times \mathbf{10}^{-6} \times \boldsymbol{T}^2 \times \mathbf{RH}^2\end{aligned} \quad (1)$$

where T and HI are in °F, while RH is in %. See Text S1 in Supporting Information S1 for more information about the HI formulation. Although there are various methods in the literature for calculating HI values, most of the algorithms implemented in these methods generate values that are strongly correlated (Anderson et al., 2013). Therefore, the formulation of HI shown in Equation 1 has been chosen not only because it is more consistent with the original apparent temperature equation (Anderson et al., 2013), but also because previous studies have shown that it performs well when applied in warm environments of America (Hass et al., 2016; Weinberger et al., 2018), Asia (Opitz-Stapleton et al., 2016; Sung et al., 2013), Europe (Diffenbaugh et al., 2007; Fischer & Schär, 2010) and even Africa (Diba et al., 2021; Fotso-Nguemo et al., 2021; Sylla et al., 2018).

For the analysis, values of HI were computed for each day, then sorted by ranges according to the categories defining the level of heat risk attributed to each range, as well as the health problems that may result as presented in Table 1. In fact, the categories are classified in the increasing scale of impact as follows: Safe, Caution, Extreme Caution (Ex-Caution), Danger and Extreme Danger (Table 1). Hence, as we move from the Caution to the Extreme Danger categories, it is possible for the human body to develop certain health problems such as fatigue, heat cramps, heat exhaustion, and/or heat stroke that can occur with prolonged exposure and/or physical activity (Lucas et al., 2014; Scovronick et al., 2018). Please visit the website "https://www.weather.gov/safety/heat-index," for more information about the HI classification and their associated health problems.

In this study, exposure is defined as the size of population be exposed to heat stress, and is computed at each grid point by multiplying the total number of occurrences of these heat events and population together for both baseline and future periods. Furthermore, the total change in exposure (in person-events) will be investigated based on the approach developed by Jones et al. (2015) and adopted by certain authors (e.g., Ayugi et al., 2022; Liu et al., 2017; Weber et al., 2020), through the following equation:

$$\Delta \boldsymbol{E} = \boldsymbol{P_R} \times \Delta \boldsymbol{C} + \boldsymbol{C_R} \times \Delta \boldsymbol{P} + \Delta \boldsymbol{C} \times \Delta \boldsymbol{P} \quad (2)$$

where $\boldsymbol{P_R}$ and $\boldsymbol{C_R}$ are the population and climate (the total number of occurrence of heat stress events) in the reference period, respectively; while $\Delta \boldsymbol{C}$ and $\Delta \boldsymbol{P}$ the climate and population changes, respectively. In Equa-

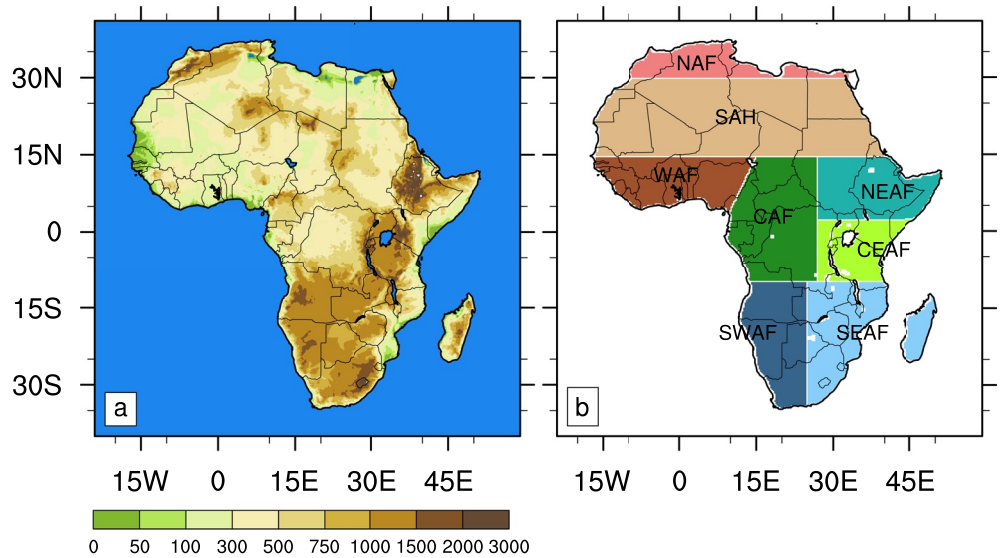

Figure 1. (a) African domain and its topography (shaded, in meters). (b) Analysis subregions, denoted as North Africa (NAF), Sahara (SAH), West Africa (WAF), Central Africa (CAF), North-East Africa (NEAF), Central-East Africa (CEAF), South-West Africa (SWAF), and SouthEast Africa (SEAF).

tion 2, the term $\boldsymbol{P_R} \times \Delta \boldsymbol{C}$ refers to the climate effect, which takes into account the influence of climate exposure; the term $\boldsymbol{C_R} \times \Delta \boldsymbol{P}$ represents the population effect; and the term $\Delta \boldsymbol{C} \times \Delta \boldsymbol{P}$ refers to the interaction effect which measures the simultaneous variations in both climate and population.

All our analysis is done over the whole African domain (Figure 1a), as well as the different subregions based on the new updated IPCC reference regions for the African continent (Iturbide et al., 2020), represented in Figure 1b as follows: North Africa (NAF), Sahara (SAH), West Africa (WAF), Central Africa (CAF), North-East Africa (NEAF), Central-East Africa (CEAF), South-West Africa (SWAF), and South-East Africa (SEAF). Changes in the area extent of each of the different HI categories are expressed as percent of the total area extent of the study domain, with only land-grid taken into account. With regard to changes on the total exposure, they will be expressed in person-events. Note that, in order to ensure that our results reflect a better analysis of the best and worst scenarios, we consider a scenario of strict emissions mitigation, combined with a low population growth scenario (RCP2.6/SSP1), as well as a scenario dominated by adaptation and mitigation challenges (RCP8.5/SSP5).

For the computation of the absolute values of these metrics during the current climate, we will consider T and RH fields from the ERA5 reanalysis data (Hersbach et al., 2020), available from 1979 to present at horizontal resolution of about 28 km (~0.25°). In order to take into account the uncertainties that may exist in the projected changes, the climate change signal from the RCMs ensemble-mean will be considered significant if at least 7 out of 9 (i.e., about 77.78%) RCMs members agree on the sign of the change. The conformity between the spatial resolution of the different data sets was ensured by remapping them onto the ERA5's reanalysis grid through the bilinear interpolation method.

3. Results

3.1. Projected Spatial Extent of Heat Stress

Figure 2 displays the spatial distribution of annual HI categories for the baseline period (ERA5 reanalysis and historical), and the different global warming scenarios over Africa. During the baseline period, ERA5 reanalysis shows a predominance of areas with moderate heat risk (Ex-Caution) in the northern part of the domain, except during the December-February where this part of the continent is dominated by areas with low (Caution) and extremely low (Safe) heat risks (Figure S1 in Supporting Information S1). Some small hotspots more or less isolated with high heat risk (Danger) are also recorded over certain countries of WAF and SAH subregions. On the other hand, the southern part of the continent is dominated by areas with low (Caution) and extremely low (Safe) heat risks, The RCMs ensemble-mean historical show a similar pattern to that of the ERA5 reanalysis but with lower heat load around mountainous areas of the studied domain. It is worth recognizing that GCMs and

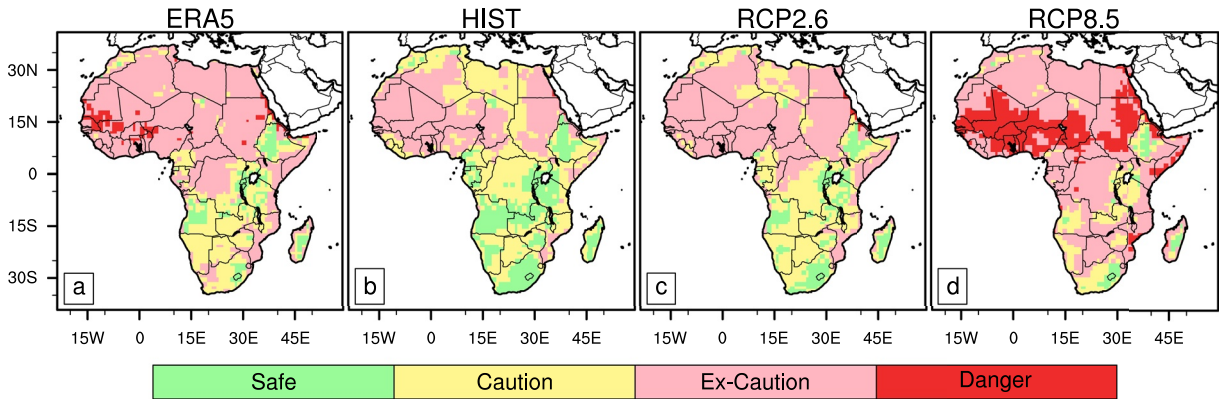

Figure 2. Spatial distribution of annual heat stress categories, during the baseline period (1979–2008) from ERA5 (first column) and historical (second column); and the late 21st century (2069–2098), under the radiative forcing scenarios RCP2.6 (third column) and RCP8.5 (fourth column).

RCMs have some deficiencies (usually characterized by systematic biases) in the representation of climate variables due to the parameterization of some processes. Therefore, the absolute values of the climate variables are most often biased, which can be seen in the differences between the baseline period of the ERA5 reanalysis data (considered here as reference fields) and the historical simulations (Figures 2a and 2b). Nevertheless, the results presented here can be considered as a rough estimate of future changes.

Compared to the baseline period, the results from the two RCPs show a progressive extension of areas with dangerous heat risks, which will be more widespread for the high GHG-forcing scenario RCP8.5. More specifically, in the case of RCP2.6, the total area with Caution and Safe conditions gradually decreases by about 9% and 10% respectively, and leave place to an extension of areas with Ex-Caution conditions, which records an increase of about 15% and the danger areas increase by about 2% (Figure S2 in Supporting Information S1). It is worth to note that by the late 21st century, the implementation of adaptation and mitigation measures in countries such as Ethiopia, Tanzania, Zambia, South Africa, and Madagascar could contribute to a slight increase of areas with Safe conditions at the disadvantage of those of Caution. Furthermore, although the lower scenario RCP2.6 is the most optimistic, several countries located in the northern part of the domain, as well as those located along the coastal area of the Indian Ocean will still be affected by Ex-Caution conditions, particularly during the March-November period (Figure S1 in Supporting Information S1).

Concerning the case of RCP8.5, which is the most pessimistic, the models project a stronger extension of Ex-Caution areas toward the southern extremity of the continent, with an increase of about 20% compared to the baseline period (Figures S1 and S2 in Supporting Information S1). In addition, the intensification of the latter heat conditions under the effect of increased global warming leads to the emergence of Danger conditions over most of West, Central and East African countries, as well as over coastal areas of the Red Sea and Indian Ocean. Consequently, in the absence of adaptation and mitigation policies, the Danger category is likely to increase by about 23% in surface area by the end of the century compared to the baseline period (Figure S2 in Supporting Information S1).

Although sometimes of smaller spatial extent, the RCMs ensemble-mean detect future climate shifts toward warmer conditions in RCP8.5 compared to RCP2.6. For instance, mountainous areas of Cameroon, Ethiopia and Angola and Great Lakes region, which were unexposed under RCP2.6, will be affected by Caution category in RCP8.5 (see Figures 2b and 2c). Moreover, we note that areas with HI of Danger category which were almost absent in RCP2.6 will significantly increase in RCP8.5 (Figure 2, Figures S1 and S2 in Supporting Information S1).

3.2. Projected Seasonal Cycles of Heat Stress

The seasonal cycles of both observed and projected HI for each subregion (Figure 1b) are presented in Figure 3. Generally, the annual evolution of HI shows peaks (with magnitude varying according to the considered GHG-emission scenario), appearing once or twice during the year, indicating the period where populations experience high heat load. During the baseline period, the seasonal cycles of HI shown by ERA5 reanalysis (purple lines) generally present peaks of moderate heat risks (with peaks between 35°C and 41°C) over the subregions

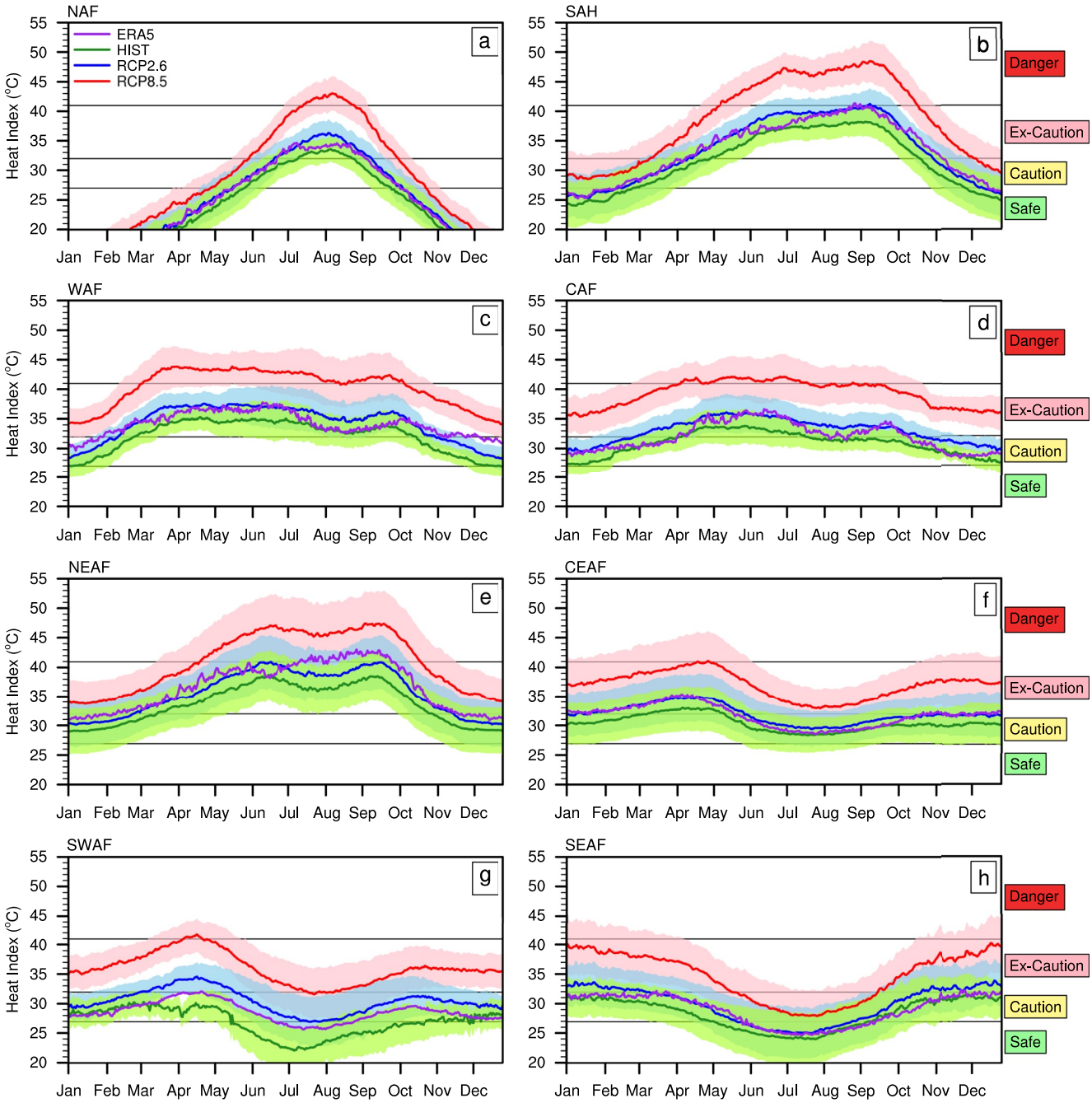

Figure 3. Seasonal cycle of regional heat index (in °C), during the baseline period (1979–2008) from ERA5 (purple) and historical (HIST; green); and the late 21st century (2069–2098), under the radiative forcing scenarios RCP2.6 (blue) and RCP8.5 (red). Green, blue and red shadings correspond to the full range of individual Regional Climate Models members for the historical, RCP2.6 and RCP8.5, respectively.

located around and northern Equator (Figures 3a–3f), except over NEAF where the presence of areas with high risk level along the Red Sea (Figure 2a) generates a peak of about 43°C around September. On the other hand, the seasonal cycles HI generally present peaks of low heat risks (with peaks up to 32°C) over the subregions located southern Equator (Figures 3g and 3h). Note that despite the high magnitude of HI over NAF during July-September, almost the entire year is dominated by heat conditions similar to that of SWAF and SEAF (i.e., Safe and Caution categories). Similar to the case of the spatial distribution of HI categories, the seasonal cycles of HI presented by the RCMs ensemble-mean historical (green lines) is similar to that of the ERA5 reanalysis but with less strong heat load, more pronounced over NEAF and SWAF.

Results from the RCP2.6 scenario show that the RCMs ensemble-mean project heat peaks localized around the same months as those found during the baseline period, but with slightly higher magnitudes (with an increase of about 4%–9% compared to the baseline period; see Figure S3 in Supporting Information S1). This difference is more noticeable in the sub-regions located in the southern part of the continent, where the slight extension of the Caution and Ex-Caution areas would lead to peaks of up to 34°C during April-May (December-February) over SWAF (SEAF). Nevertheless, this increase could have as main consequence the intensification of heat load toward higher heat magnitudes, coupled with a slight extension of period of discomfort due to heat.

With regard to the high emissions scenario RCP8.5, the RCMs ensemble-mean suggests a substantial increase in HI values, with magnitudes largely exceeding the thresh old of high risk (41°C) over SAH (with peak of about 49°C during September-October) and NEAF (with peak of about 47°C during June-July and September-October). According to this scenario, the magnitude of HI is projected to increase by about 10%–29% with respect to the baseline period, over all subregions (Figure S3 in Supporting Information S1). This could be translated by an intensification of heat stress toward heat conditions of high-risk level, and lengthening of periods of Ex-Caution over all subregions.

It is important to note that with the increased global warming toward the high emission scenarios, areas such as NAF, SAH, WAF, CAF, and NEAF are likely to experience the emergence of HI of Danger category, with relatively high magnitudes compared to the case of low emission scenarios Therefore, an increase of about 6%–20% is recorded over these subregions when going from RCP2.6 to RCP8.5. Furthermore, the duration of these dangerous heat periods will differ according to the subregions, ranging from two consecutive months (July-September) over NAF, to seven consecutive months (March-October) over WAF.

3.3. Projected Total Number of Days of Occurrence of Heat Stress

Figure 4 shows the projected changes in the total number of days per year with each HI categories, for the different global warming scenarios over Africa. Changes in the number of days with Safe conditions presents a generalized decrease over the entire domain, with peaks more pronounced for RCP8.5 (up to 350 days/year) over countries located around the Equator (between 15°S and 15°N; see Figures 4a and 4b). In fact, areas such as Sierra Leone, Liberia, southern Cameroon, Central African Republic, Gabon, Congo, northern Angola, DRC, and Uganda, which present a strong decreases in Safe conditions, are those likely to experience more number of days with Caution heat conditions. Furthermore, areas where there is almost no change in this heat condition (northern Morocco, northern Algeria, western Cameroon, Burundi, central Ethiopia, western Kenya, central Angola, eastern South Africa including Lesotho), correspond to countries experiencing almost no heat stress throughout the year, with a number of days with Safe conditions reaching 350 days/year (see Figures S4a–S4c in Supporting Information S1).

Regarding the future evolution of HI of Caution category, we note an increase in its number of days of occurrence, with peaks of up to 200 and 300 days/year for RCP2.6 and RCP8.5 respectively, over countries located between the 30°S and 10°N band (Figures 4c and 4d). Furthermore, we note a significant decrease in the number of days with this category over countries located between 5° and 20°N, which persists and becomes more pronounced with increasing global warming (with decrease of up to 100 and 200 days/year for RCP2.6 and RCP8.5 respectively).

The number of days with Ex-Caution conditions shows a generalized increase over most of the northern part of the continent, with peaks located around the Equator (between 10°S and 20°N; see Figures 4e and 4f). For this category, which may represent a moderate risk level to local populations, their number of days of occurrence is almost 5-fold compared to the baseline period, with a projected peak of about 50% and 250% for RCP2.6 and RCP8.5 respectively over WAF, CAF, and NEAF.

Although with a small spatial extent, the RCMs ensemble-mean project an extension of the number of days with Danger heat conditions over some countries included in WAF and NEAF, only for high emission scenarios. Therefore, populations of countries located in these subregions are likely to experience about 20–50 days/year with high heat-risk level (Figure S4i in Supporting Information S1).

3.4. Projected Population Exposure to Heat Stress

Exposure to future heat stress generally depends on future population changes occurring in a given country, including adopted urbanization planning, population growth, as well as their vulnerability. For the African

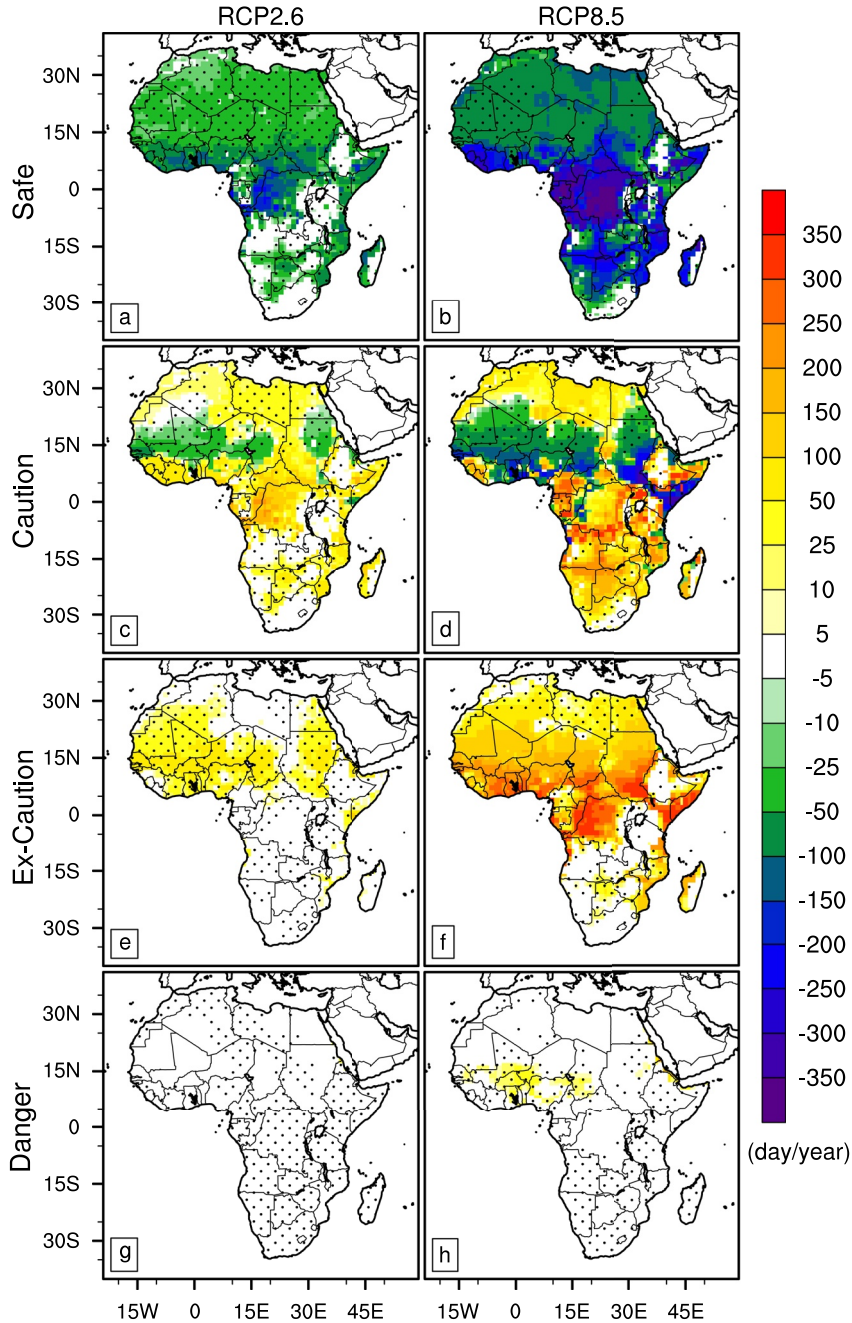

Figure 4. Spatial distribution of change in the total number of days of occurrence (with respect to the 1979–2008 historical data; in day per year) of each heat stress categories, during the late 21st century (2069–2098), under the radiative forcing scenarios RCP2.6 (first column) and RCP8.5 (second column). Dots indicate areas where the change is significant (i.e., where at least 7 out of 9 Regional Climate Models members agree on the sign of the change).

continent in particular, the results showed that during the baseline period, the exposure to hazardous heat stress conditions is relatively low (Figure S6 in Supporting Information S1), probably due to not only the very few number of occurrence of such events in some densely populated areas (e.g., NAF, CAF, NEAF, SEAF, SWAF, and SEAF; Figure S4 in Supporting Information S1), but also to its moderate demography during that period (Figure S5 in Supporting Information S1).

The spatial distribution of the total exposure change for each HI category and for the different considered global warming scenarios over Africa, is presented in Figure 5. The spatial variation of total exposure to Safe category is generally high over the entire domain, except over SAH, SWAF, and some parts of CAF where less than 1 million

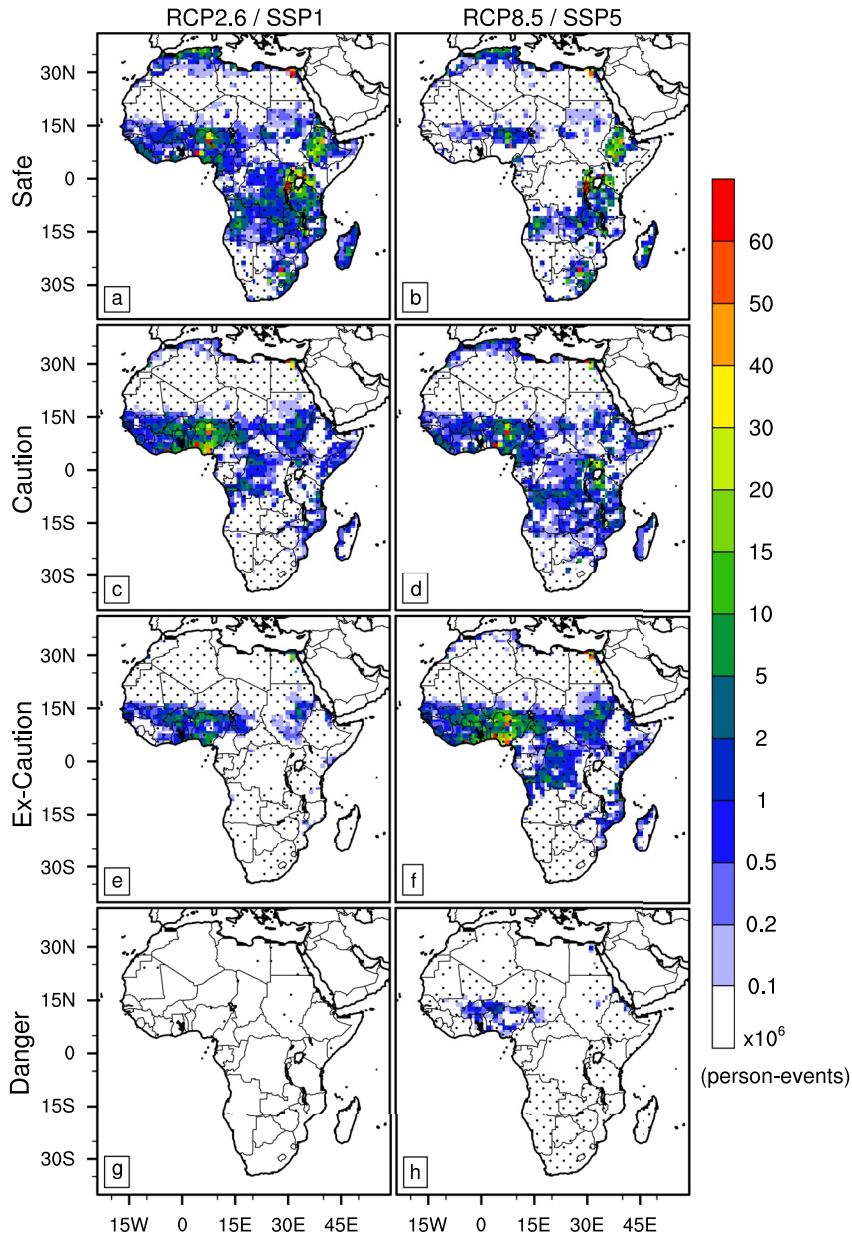

Figure 5. Spatial distribution of total change in exposure (with respect to the 1979–2008 historical data; in 10^6 person-events) to each heat stress categories, during the late 21st century (2069–2098), under the radiative forcing scenarios RCP2.6/SSP1 (first column) and RCP8.5/SSP5 (second column). Dots indicate areas where the change is significant (i.e., where at least 7 out of 9 Regional Climate Models members agree on the sign of the change).

person-events will experience extremely low heat conditions under both considered scenarios. Concerning the HI with Caution conditions, pattern of the total exposure is similar to that of Safe, but with a wider spatial extent as the GHG-forcing scenario increases. Here, the highest value of the regional change in the total exposure is observed over WAF, where about 6.5 and 2.5 million person-events are likely to experience low heat conditions under RCP2.6/SSP1 and RCP8.5/SSP5 respectively (Figures 6c and 6d). For this heat category, the population effect seems to be the main driver of the total change over all subregions, except for SWAF and SEAF where the interaction effect contributes for about 83% and 67%, respectively to the total exposure change under RCP8.5/SSP5 (Figure 6 and Table S2 in Supporting Information S1; Caution).

The total change in exposure to heat with Ex-Caution conditions is smaller than that of the two previous HI categories and is generally confined in the subregions located around the Equator (between 15°S and 15°N;

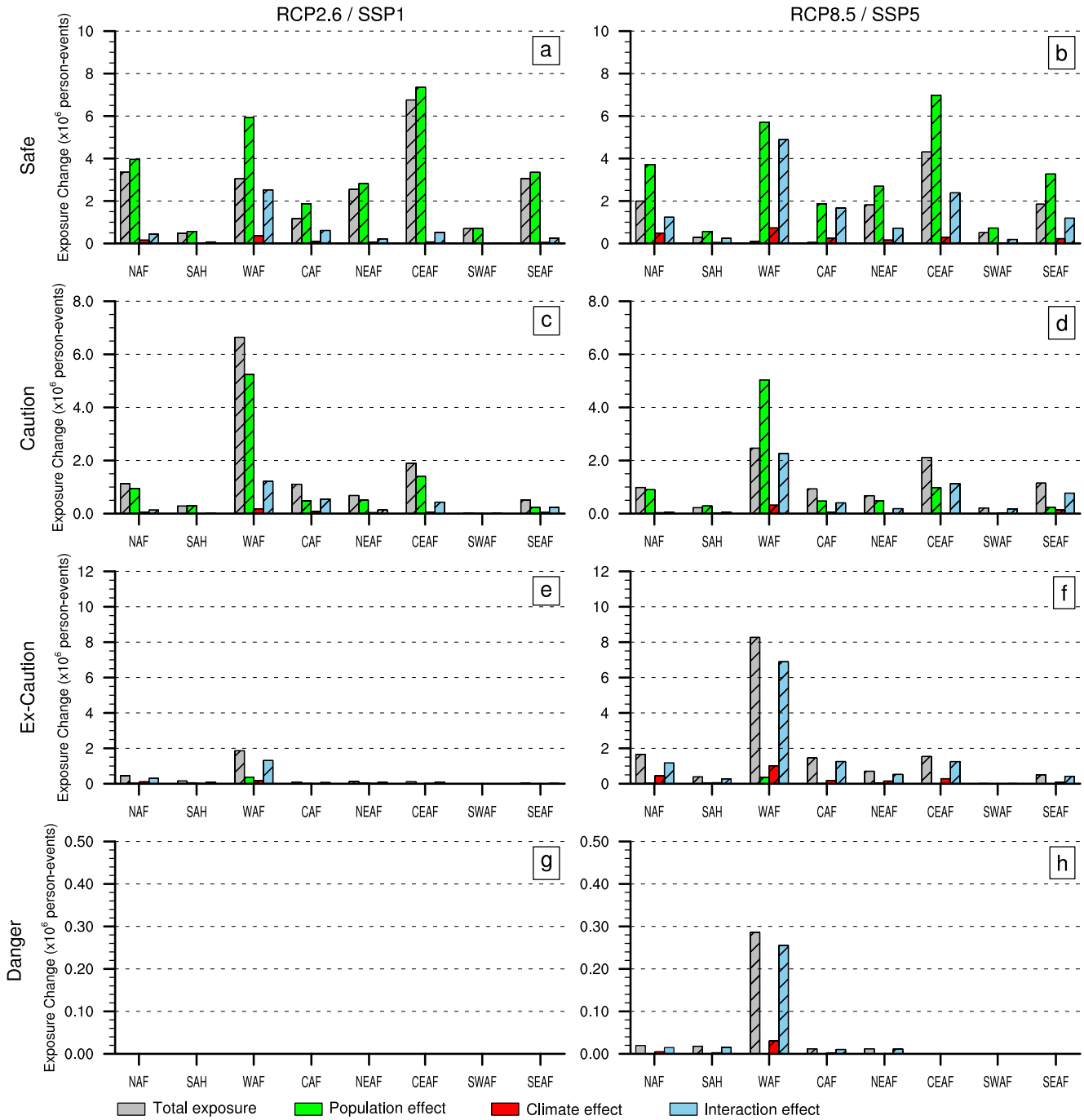

Figure 6. Regional mean of total change in exposure (with respect to the 1979–2008 historical data; in 10^6 person-events) to each heat stress categories and the contribution of different drivers (population, climate, and population-climate interaction), during the late 21st century (2069–2098), under the radiative forcing scenarios RCP2.6/SSP1 (first column) and RCP8.5/SSP5 (second column). Diagonal lines indicate significant change (i.e., where at least 7 out of 9 Regional Climate Models members agree on the sign of the change).

Figures 5e and 5f). Furthermore, the RCMs ensemble-mean project peak of exposures more pronounced for RCP8.5/SSP5 compared to RCP2.6/SSP1, with about 40–60 million person-events at risk over Côte d'Ivoire (with hotspot in Abidjan), Nigeria (with hotspots in Lagos, Port-Harcourt and Kano) and Egypt (with hotspot in Cairo). In the case of this heat condition, the interaction effect is found to be the main driver of this change, with contributions of about 85% (CEAF) and 87% (SWAF) under RCP2.6/SSP1 and RCP8.5/SSP5 respectively (see Figure 6 and Table S2 in Supporting Information S1; Ex-Caution). For the risk category Danger, the RCMs

ensemble-mean project a moderate spatial pattern, with about 1–2 million person-events at risk over Burkina Fao (with hotspot in Ouagadougou), Ghana (with hotspot in Abidjan), southern Niger (with hotspot in Bolgatanga), and Nigeria (with hotspots in Bimming Kebbi, Port-Harcourt and Kano). In this case, the interaction effect seems to be the main driver of change with a contribution of about 95% over NEAF (Figure 6 and Table S2 in Supporting Information S1; Danger).

4. Discussion

Our results suggest that for both RCP2.6 and RCP8.5 scenarios, countries located around the Equator (between 15°S and 15°N) are likely to experience substantial increases in heat stress by the end of this century.

Particularly, analysis of the future evolution of the spatial extent of heat stress categories revealed that the RCMs ensemble-mean project a predominance of Safe and Caution heat conditions in the southern part of the domain, for which spatial extent gradually decreases as global warming increases (with a decrease of up to 25% under RCP8.5). The relatively low heat conditions that are still present around the mountainous areas even under the RCP8.5 scenario would probably be related to the small changes in both temperature and RH generally observed around these high terrain features as shown in Fotso-Nguemo et al. (2021). We further noted a strong extension of Ex-Caution (Danger) conditions, which would increase by 20% (23%) under RCP8.5 against an increase of 15% (2%) under RCP2.6 over the continent, and will affected most countries of SAH, WAF, CAF, and NEAF subregions. This implies that in the case of Ex-Caution (Danger) heat category, the increase in global warming would induce a 4-fold (12-fold) increase in the area affected by dangerous heat conditions. Although restricted to a subregional scale, the future evolution of the spatial extent of high heat stress conditions has been investigated by other authors (e.g., Fotso-Nguemo et al., 2021; Sylla et al., 2018), who have also concluded to an increase under the effects of increased global warming levels. Accordingly, the study conducted over WAF by Sylla et al. (2018) showed an almost 1.5-fold increase in the spatial extent of Ex-Caution heat category, for the global warming levels ranging from 1.5°C to 2°C under RCP8.5. Similarly, the study Fotso-Nguemo et al. (2021) realized over CAF, showed a 3-fold increase in the spatial extent of Ex-Caution heat category, for global warming levels ranging from 1.5°C to 3°C under RCP8.5.

The projected seasonality of heat stress showed that populations from certain subregions of Africa, especially those located around the Equator (SAH, WAF, CAF, and NEAF) could experience a tendency toward not only an increase in magnitude, but also in the number of months of high heat-related risk under RCP8.5 compared to RCP2.6. This trend toward higher heat conditions over these subregions of the continent is probably induced by the projected increase in temperature which would occurs as the result of anthropogenic land use and land cover modification. In fact, the increasing demand for cropland could leads to a decrease in vegetation cover and consequently to a decrease in evapotranspiration, moisture convergence and surface roughness (Halder et al., 2015; Roy et al., 2022) which contribute to the modulation of heat stress. Furthermore, the results showed that compared to the northern part of the continent, the projected seasonality of heat stress has moderate values over southern Africa (SWAF and SEAF), with low heat categories experienced especially during the dry season (June-September) even under the RCP8.5 scenario. This heat stress behavior observed during the dry season could be explained by the increasing practice of irrigation activity over some economically advanced countries of this subregion. Indeed, the increase in irrigation activity on cropland could compensate for the increase in thermal gradients caused by land conversion, as irrigation provides an alternative source of soil moisture, and thus lowers surface temperature through evaporation (Halder et al., 2015; Prijith et al., 2021; Roy et al., 2022). The results found here are consistent with the studies of Asefi-Najafabady et al. (2018) and Jagarnath et al. (2020), where in their study areas (CEAF and SEAF, respectively) have shown a trend toward not only a lengthening of the periods of high heat felt by population, but also an intensification of their magnitude. Our results show that the subregion with the longest duration of high heat-related risk is WAF, with up to seven consecutive months (March-October) of Danger heat category under RCP8.5. Similarly, the subregion with the strongest heat events is SAH, with a HI of 49°C around September under RCP8.5, representing an increase of about 8°C when moving from RCP2.6 to RCP8.5. Overall, an increased magnitude of about 6%–20% is recorded over the above subregions when moving from RCP2.6 to RCP8.5.

Concerning changes in the number of days of occurrence of each heat stress categories, we noted an almost 4-fold increase in the number of days with Ex-Caution conditions, with a projected peak of about 60% and 15% of the length of the year for RCP8.5 and RCP2.6 respectively, over WAF, CAF, and NEAF. The increase of number

of heat stress events due to increased radiative forcing will contribute to the emergence of dangerous heat stress conditions, for which the number of days will increase by about 10%–30% at the end of the century. These events mostly concern countries such as Senegal, Mali, Burkina Faso, Ghana, Benin, Niger, Nigeria, Cameroon and Chad, Sudan, Ethiopia, Somalia, Eritrea, and Egypt. These results suggest a significant transformation of the heat environments of the concerned countries, since greater occurrences of hot days could have disastrous consequences for the health of their populations and thus for their income-generating activities. Substantial increase in the number of days of occurrence of extreme heat events over Africa has also been recently reported by certain authors (e.g., Asefi-Najafabady et al., 2018; Diba et al., 2022; Diedhiou et al., 2018; Fotso-Nguemo et al., 2021; Jagarnath et al., 2020; Sylla et al., 2018; Weber et al., 2020; Yengoh & Ardö, 2020), indicating that future heat hazard conditions will worsen in the future if no mitigation efforts are implemented. However, the projections of the number of days of occurrence of Extremely Low heat conditions for late 21st century could allow to anticipate on the locations where demographic transitions are most likely to occur. For instance, the mountainous areas of Morocco, western Cameroon, Ethiopia, Angola, South Africa, eastern Madagascar, and the Great Lakes region are likely to be unaffected by heat-related risks whatever the considered radiative forcing scenario.

The analysis of change in population exposure to heat conditions showed that the areas exposed to extremely low heat-related risk levels were more widespread and strong for RCP2.6/SSP1 than for RCP8.5/SSP5. This suggests that the climate change has the effect of reducing the spatial extent of thermal comfort areas, for which peaks of about 60 million person-events are localized over the mountainous regions of Nigeria, Rwanda, Burundi, and Ethiopia (see Figures 5a and 5b). The highest value of the regional change in total exposure is thus recorded over CEAF, where about 7 and 4.5 million person-events are likely to experience Safe heat conditions under RCP2.6/SSP1 and RCP8.5/SSP5, respectively (Figures 6a and 6b). The results also reveal that the subregion in which populations will be most exposed to high heat-related risk levels is WAF, for which th majority of countries currently remain highly vulnerable to the adverse effects of climate change due to due to several factors, including: (a) the rapidly growing populations; (b) the relatively low adaptive capacity; and (c) scarce of cooling infrastructures. This result was found for the both considered scenarios, with the RCMs ensemble-mean projecting a regional change of about 2 and 8.5 million person-events respectively, likely to experience Ex-Caution heat conditions under RCP2.6/SSP1 and RCP8.5/SSP5 respectively (Figures 6e and 6f). This means that in this particular subregion, the increase of radiative forcing would lead to a about 4-fold increase in exposure to moderate heat stress, which exacerbation could potentially induce the exposure of about 300,000 person-events to Danger heat-related risks level under RCP8.5/SSP5 (Figure 6h).

Currently, it is difficult to explain with precision the driven mechanisms responsible for these changes. However, some important factors such as (a) large-scale variability through atmospheric parameters (insulation, temperature, precipitation, humidity, cloud cover); (b) changes in anthropogenic GHG concentrations; and (c) changes in land use and land cover could play a key role (Coffel et al., 2018; Pal & Eltahir, 2016). Nevertheless, in order to understand the relative importance of the potential drivers of projected changes in population exposure to high heat stress, results of the total change in exposure were divided into three components (climate, population, and interaction effects). It thus appears that for both considered scenarios, the population effect appears to be dominant in explaining the total changes in exposure due to extremely low (Safe) and low (Caution) heat-related risks over most subregions of the African continent. Concerning the total changes in exposure to moderate (Ex-Caution) and high (Danger) heat-related risks, the interaction effect between climate change and population growth appears to be one of the dominant drivers. This result is in agreement with the findings of Liu et al. (2017), who in their study conducted with 5 GCMs showed that the total changes in exposure to extreme heat over several regions of the world including Africa, was mainly caused by the synergistic interaction between the large increases in the number of high-heat days during the year and rapidly increasing population. It is worth pointing out that apart from the interaction effect, although of small proportion, the population (climate) effect also plays a role in the case of scenario RCP2.6/SSP1 (RCP8.5/SSP5).

Note that, although the heat stress category of extreme danger conditions does not appear in the considered HI climatology, it cannot be excluded that it may occur on certain days, both during the baseline period and in future GHG-forcing scenarios. Moreover, whilst we used the high-resolution CORDEX-CORE projections data set, their ensemble-mean size is not sufficiently robust (only nine members derived from three RCMs). This is likely to provide a limited quantification of the uncertainty associated with the projected HI. Therefore, different results would be expected by considering, for example: (a) other algorithms for computing heat index; (b) the type of

model used to estimate the heat index as well as the population growth; (c) a larger RCMs ensemble-mean; and (d) aerosol variation as well as deforestation/afforestation scenarios.

5. Conclusion

The aim of this research was to explore the response of increased anthropogenic radiative forcing on heat stress changes over the African continent toward the late 21st century, not only in terms of its spatial extent, seasonality and number of days of occurrence, but also in terms of the number of person likely to be exposed to these extreme heat events. For this purpose, we have considered the projections of HI computed based the United States National Weather Service's algorithm (Rothfusz, 1990) applied to an ensemble-mean of high-resolution RCMs, performed in the framework of the CORDEX-CORE initiative; combined with projections of population growth from ISIMIP2b (only for the baseline period) and SEDAC data sets.

Our results suggest that for all heat stress categories susceptible to create discomfort to populations, their projected changes would be stronger in the high-emission scenario than in that of low-emission. It was shown that in the future, heat conditions of high-risk category will be more severe for populations living over subregions such as SAH, WAF, CAF, and NEAF, especially if no adaptation and mitigation policies are implemented. The simultaneous effects of population growth and increasing global warming has been identified as one of the drivers of this trend toward more spatially and temporally widespread heat events. Recent studies have shown that prolonged exposure to such heat conditions could lead to certain health problems such as heat cramps, heat exhaustion and even heat stroke following a prolonged physical activity (Lucas et al., 2014; Scovronick et al., 2018). Besides the direct negative health impacts, socio-economic sectors that are essential for the development of countries of these subregions could also be affected, through reduced availability and productivity of outdoor workers (e.g., agro-pastoral, fishing, construction, transport, industries, firefighter, services, etc.), or disruptions in the electrical network due to high demand for electrical energy to cool down (Parkes et al., 2019; Sylla et al., 2018; Yengoh & Ardö, 2020). Therefore, the projected high heat stress, coupled with the existing problems in most developing countries (e.g., poverty, weak institutions, political unrest, etc.), will further increase the vulnerability of affected countries. These potential threats could justify the need to urgently implement practices that will allow not only to strongly mitigate the effects of increased radiative forcing, but also to sustainably adapt populations living in affected countries for dealing with a warming world, even in regions considered not to be at risk during the baseline period.

For instance, there is still a need for further research to accurately specify the most appropriate measures for populations of the affected areas, nevertheless some actions can be envisaged by public authorities and/or even when possible by the concerned individuals.

- The establishment of a heat index-based health prevention plan for populations, with a particular focus on outdoor workers. The purpose of such a plan would be to prevent heat-related illnesses and even deaths by, for example, raising awareness among workers and decision-makers about health problems associated with working in hot environments (Coffel et al., 2018; Yengoh & Ardö, 2020);
- Develop and disseminate protective strategies for workers who often work outdoors in adverse weather conditions. These measures could help to reduce heat-related mortality by providing recommendations on: the setting of work and rest schedules, choosing appropriate clothes for different heat stress circumstances, the choice of foods to avoid (e.g., proteins, alcohol, etc.) and to prioritize (e.g., fruits, vegetables, etc.) in order to keep metabolic heat at a reasonable level, adopting cooling strategies according to social level, the importance of hydration during working hours and how to deal with heat-related emergencies, among others (Coffel et al., 2018; Yengoh & Ardö, 2020);
- Encouraging and disseminating good practices in order to reduce anthropogenic GHG-forcing and thus temperature. Having the lower temperatures would reduce the number of high heat stress events which can result in lower costs of adapting the energy system to climate change and thus provide enough electricity to prevent heat stress through the cooling of the local environment (Akara et al., 2021; Parkes et al., 2019).

Data Availability Statement

The CORDEX-CORE data sets used in this research are available through the ESGF website "https://esg-dn1.nsc.liu.se/search/cordex/; https://esgf-data.dkrz.de/projects/esgf-dkrz/." Furthermore, the ISIMIP2b data sets can be downloaded through the website "https://www.isimip.org/gettingstarted/details/31." Moreover, the SEDAC data

sets can be retrieved through the link "https://sedac.ciesin.columbia.edu/data/set/popdynamics-1-8th-pop-base-year-projection-ssp-2000-2100-rev01/data-download." Finally, the ERA5 reanalysis data sets are available through the website "https://cds.climate.copernicus.eu/cdsapp#!/dataset/reanalysis-era5-single-levels?tab=form."

Acknowledgments
The first author gratefully acknowledges all researchers of GERICS for their close collaboration during his stay at Hamburg. Furthermore, the authors would like to thank the German Climate Computing Center (DKRZ) in Hamburg for providing the high-computing capacity. The National Computing Center of Côte d'Ivoire (CNCCI) is also acknowledged for its support through the granting of access to its facilities. We would also like to thank the climate modelling groups listed in Table S1 in Supporting Information S1 for producing and making their model output freely available through the Earth System Grid Federation's (ESGF) platforms "https://esgf-data.dkrz.de/projects/esgf-dkrz/." We also acknowledge the Inter-Sectoral Impact Model Intercomparison Project (ISIMIP2b) and the NASA Socioeconomic Data and Applications Center (SEDAC) for providing the historical and projected population growth data sets. Thanks are also expressed to the Copernicus Climate Change Service (C3S) for providing the ERA5 reanalysis data sets. Finally, the authors gratefully acknowledge the efforts of the two anonymous reviewers, along with those of colleagues from GERICS for their recommendations and suggestions, which have greatly helped in improving and clarifying the initial version of the manuscript. This research was supported by the DAAD within the framework of the climapAfrica program with funds of the Federal Ministry of Education and Research (Grant 57516494). The publisher is fully responsible for the content. Open Access funding enabled and organized by Projekt DEAL.

References

Akara, G. K., Hingray, B., Diawara, A., & Diedhiou, A. (2021). Effect of weather on monthly electricity consumption in three coastal cities in West Africa. *AIMS Energy*, *9*(3), 446–464. https://doi.org/10.3934/energy.2021022

Anderson, G. B., Bell, M. L., & Peng, R. D. (2013). Methods to calculate the heat index as an exposure metric in environmental health research. *Environmental Health Perspectives*, *121*(10), 1111–1119. https://doi.org/10.1289/ehp.1206273

Asefi-Najafabady, S., Vandecar, K. L., Seimon, A., Lawrence, P., & Lawrence, D. (2018). Climate change, population, and poverty: Vulnerability and exposure to heat stress in countries bordering the Great Lakes of Africa. *Climate Change*, *148*(4), 561–573. https://doi.org/10.1007/s10584-018-2211-5

Ayugi, B., Jiang, Z., Iyakaremye, V., Ngoma, H., Babaousmail, H., Onyutha, C., et al. (2022). East African population exposure to precipitation extremes under 1.5°C and 2.0°C warming levels based on CMIP6 models. *Environmental Research Letters*, *17*(4), 1–15. https://doi.org/10.1088/1748-9326/ac5d9d

Bouwer, L. M. (2013). Projections of future extreme weather losses under changes in climate and exposure. *Risk Analysis*, *33*(5), 915–930. https://doi.org/10.1111/j.1539-6924.2012.01880.x

Burkart, K., Khan, M. M. H., Schneider, A., Breitner, S., Langner, M., Kraemer, A., & Endlicher, W. (2014). The effects of season and meteorology on human mortality in tropical climates: A systematic review. *Transactions of the Royal Society of Tropical Medicine and Hygiene*, *108*(7), 393–401. https://doi.org/10.1093/trstmh/tru055

Ciarlò, J. M., Coppola, E., Fantini, A., Giorgi, F., Gao, X., Tong, Y., et al. (2021). A new spatially distributed added value index for regional climate models: The EURO-CORDEX and the CORDEX-CORE highest resolution ensembles. *Atmosphere*, *10*(5–6), 1403–1424. https://doi.org/10.1007/s00382-020-05400-5

Coffel, E. D., Horton, R. M., & De Sherbinin, A. (2018). Temperature and humidity based projections of a rapid rise in global heat stress exposure during the 21st century. *Environmental Research Letters*, *13*, 1–9. https://doi.org/10.1088/1748-9326/aaa00e

Colin, J. (2011). *Étude des évènements précipitants intenses en méditerranée: Approche par la modélisation climatique réginale* (Thèse de doctorat, Vol. 35). Université Paul Sabatier.

Diallo, I., Giorgi, F., Deme, A., Tall, M., Mariotti, L., & Gaye, A. T. (2016). Projected changes of summer monsoon extremes and hydroclimatic regimes over West Africa for the twenty-first century. *Climate Dynamics*, *47*(12), 3931–3954. https://doi.org/10.1007/s00382-016-3052-4

Diallo, I., Giorgi, F., & Stordal, F. (2018). Influence of Lake Malawi on regional climate from a double-nested regional climate model experiment. *Climate Dynamics*, *50*(9–10), 3397–3411. https://doi.org/10.1007/s00382-017-3811-x

Diba, I., Basse, J., Ndiaye, M., Sabaly, H., Diedhiou, A., & Camara, M. (2021). Potential dust induced changes on the seasonal variability of temperature extremes over the Sahel: A regional climate modeling study. *Frontiers of Earth Science*, *8*, 1–18. https://doi.org/10.3389/feart.2020.591150

Diba, I., Diedhiou, A., Famien, A. M., Camara, M., & Fotso-Nguemo, T. C. (2022). Changes in compound extremes of rainfall and temperature over West Africa using CMIP5 simulations. *Environmental Research Communications*, *4*(10), 1–12. https://doi.org/10.1088/2515-7620/ac9aa7

Diedhiou, A., Bichet, A., Wartenburger, R., Seneviratne, S. I., Rowell, D. P., Sylla, M. B., et al. (2018). Changes in climate extremes over West and Central Africa at 1.5°C and 2°C global warming. *Environmental Research Letters*, *13*(6), 1–11. https://doi.org/10.1088/1748-9326/aac3e5

Diffenbaugh, N. S., Pal, J. S., Giorgi, F., & Gao, X. (2007). Heat stress intensification in the Mediterranean climate change hotspot. *Geophysical Research Letters*, *34*(11), L11706. https://doi.org/10.1029/2007GL030000

Dosio, A., Jury, M. W., Almazroui, M., Ashfaq, M., Diallo, I., Engelbrecht, F. A., et al. (2021). Projected future daily characteristics of African precipitation based on global (CMIP5, CMIP6) and regional (CORDEX, CORDEX-CORE) climate models. *Climate Dynamics*, *57*(11–12), 3135–3158. https://doi.org/10.1007/s00382-021-05859-w

Fischer, E. M., & Schär, C. (2010). Consistent geographical patterns of changes in high-impact European heatwaves. *Nature Geoscience*, *3*, 398–403. https://doi.org/10.1038/ngeo866

Forget, Y., Shimoni, M., Gilbert, M., & Linard, C. (2021). Mapping 20 years of urban expansion in 45 urban areas of sub-Saharan Africa. *Remote Sensing*, *13*(3), 1–19. https://doi.org/10.3390/rs13030525

Fotso-Kamga, G., Fotso-Nguemo, T. C., Diallo, I., Yepdo, Z. D., Pokam, W. M., Vondou, D. A., & Lenouo, A. (2020). An evaluation of COSMO-CLM regional climate model in simulating precipitation over Central Africa. *International Journal of Climatology*, *40*(5), 2891–2912. https://doi.org/10.1002/joc.6372

Fotso-Nguemo, T. C., Diallo, I., Diakhaté, M., Vondou, D. A., Mbaye, M. L., Haensler, A., et al. (2019). Projected changes in the seasonal cycle of extreme rainfall events from CORDEX simulations over Central Africa. *Climatic Change*, *155*(3), 339–357. https://doi.org/10.1007/s10584-019-02492-9

Fotso-Nguemo, T. C., Vondou, D. A., Diallo, I., Diedhiou, A., Weber, T., Tanessong, R. S., et al. (2021). Potential impact of 1.5°, 2°, and 3°C global warming levels on heat and discomfort indices changes over Central Africa. *Science of the Total Environment*, *804*, 1–11. https://doi.org/10.1016/j.scitotenv.2021.150099

Fotso-Nguemo, T. C., Vondou, D. A., Tchawoua, C., & Haensler, A. (2016). Assessment of simulated rainfall and temperature from the regional climate model REMO and future changes over Central Africa. *Climate Dynamics*, *48*(11–12), 3685–3705. https://doi.org/10.1007/s00382-016-3294-1

Giorgi, F., Coppola, E., Jacob, D., Teichmann, C., Abba Omar, S., Ashfaq, M., et al. (2022). The CORDEX-CORE EXP-I initiative: Description and highlight results from the initial analysis. *Bulletin of the American Meteorological Society*, *103*(2), E293–E310. https://doi.org/10.1175/BAMS-D-21-0119.1

Halder, S., Saha, S. K., Dirmeyer, P. A., Chase, T. N., & Goswam, B. N. (2015). Investigating the impact of land-use land-cover change on Indian summer monsoon daily rainfall and temperature during 1951–2005 using a regional climate model. *Hydrology and Earth System Sciences Discussions*, *12*, 6575–6633. https://doi.org/10.5194/hessd-12-6575-2015

Hass, A. L., Ellis, K. N., Reyes Mason, L., Hathaway, J. M., & Howe, D. A. (2016). Heat and humidity in the city: Neighborhood heat index variability in a midsized city in the southeastern United States. *International Journal of Environmental Research and Public Health*, *13*, 1–19. https://doi.org/10.3390/ijerph13010117

Hersbach, H., Bell, B., Berrisford, P., Hirahara, S., Horányi, A., Muñoz-Sabater, J., et al. (2020). The ERA5 global reanalysis. *Quarterly Journal of the Royal Meteorological Society*, *146*(730), 1999–2049. https://doi.org/10.1002/qj.3803

IPCC. (2022). Summary for policymakers. In H.-O. Pörtner, D. C. Roberts, M. Tignor, E. S. Poloczanska, K. Mintenbeck, et al. (Eds.), *Climate change 2022: Impacts, adaptation, and vulnerability. Contribution of Working Group II to the Sixth Assessment Report of the Intergovernmental Panel on Climate Change*. Cambridge University Press.

Iturbide, M., Gutiérrez, J. M., Alves, L. M., Bedia, J., Cerezo-Mota, R., Cimadevilla, E., et al. (2020). An update of IPCC climate reference regions for subcontinental analysis of climate model data: Definition and aggregated datasets. *Earth System Science Data*, *12*(4), 2959–2970. https://doi.org/10.5194/essd-12-2959-2020

Iyakaremye, V., Zeng, G., Yang, X., Zhang, G., Ullah, I., Gahigi, A., et al. (2021). Increased high-temperature extremes and associated population exposure in Africa by the mid-21st century. *Science of The Total Environment*, *790*, 148162. https://doi.org/10.1016/j.scitotenv.2021.148162

Jagarnath, M., Thambiran, T., & Gebreslasie, M. (2020). Heat stress risk and vulnerability under climate change in Durban metropolitan, South Africa-identifying urban planning priorities for adaptation. *Climate Change*, *163*(2), 807–829. https://doi.org/10.1007/s10584-020-02908-x

Jones, B., & O'Neill, B. C. (2016). Spatially explicit global population scenarios consistent with the shared socioeconomic pathways. *Environmental Research Letters*, *11*(8), 084003. https://doi.org/10.1088/1748-9326/11/8/084003

Jones, B., O'Neill, B. C., McDaniel, L., McGinnis, S., Mearns, L. O., & Tebaldi, C. (2015). Future population exposure to US heat extremes. *Nature Climate Change*, *5*(7), 652–655. https://doi.org/10.1038/NCLIMATE263

Liu, Z., Anderson, B., Yan, K., Dong, W., Liao, H., & Shi, P. (2017). Global and regional changes in exposure to extreme heat and the relative contributions of climate and population change. *Scientific Reports*, *7*, 1–9. https://doi.org/10.1038/srep43909

Lucas, R. A., Epstein, Y., & Kjellstrom, T. (2014). Excessive occupational heat exposure: A significant ergonomic challenge and health risk for current and future workers. *Extreme Physiology & Medicine*, *3*, 1–8. https://doi.org/10.1186/2046-7648-3-14

Ma, F., & Yuan, X. (2021). Impact of climate and population changes on the increasing exposure to summertime compound hot extremes. *Science of the Total Environment*, *772*, 145004. https://doi.org/10.1016/j.scitotenv.2021.145004

Medina-Ramon, M., & Schwartz, J. (2007). Temperature, temperature extremes, and mortality: A study of acclimatisation and effect modification in 50 US cities. *Occupational and Environmental Medicine*, *64*(12), 827–833. https://doi.org/10.1136/oem.2007.033175

Moss, R. H., Edmonds, J., Hibbard, K., Manning, M. R., Rose, S. K., van Vuuren, D. P., et al. (2010). The next generation of scenarios for climate change research and assessment. *Nature*, *463*(7282), 747–756. https://doi.org/10.1038/nature08823

Nikulin, G., Jones, C., Samuelsson, P., Giorgi, F., Asrar, G., Büchner, M., et al. (2012). Precipitation climatology in an ensemble of CORDEX-Africa regional climate simulations. *Journal of Climate*, *25*(18), 6057–6078. https://doi.org/10.1175/JCLI-D-11-00375.1

Opitz-Stapleton, S., Sabbag, L., Hawley, K., Tran, P., Hoang, L., & Nguyen, P. H. (2016). Heat index trends and climate change implications for occupational heat exposure in Da Nang, Vietnam. *Climate Services*, *2*, 41–51. https://doi.org/10.1016/j.cliser.2016.08.001

Opoku, S. K., Filho, W. L., Hubert, F., & Adejumo, O. (2021). Climate change and health preparedness in Africa: Analysing trends in six African countries. *International Journal of Environmental Research and Public Health*, *18*(9), 1–29. https://doi.org/10.3390/ijerph18094672

Pal, J. S., & Eltahir, E. A. (2016). Future temperature in Southwest Asia projected to exceed a threshold for human adaptability. *Nature Climate Change*, *6*(2), 197–200. https://doi.org/10.1038/nclimate2833

Parkes, B., Cronin, J., Dessens, O., & Sultan, B. (2019). Climate change in Africa: Costs of mitigating heat stress. *Climate Change*, *154*(3–4), 461–476. https://doi.org/10.1093/trstmh/tru055

Pokam, M. W., Longandjo, G. N., Moufouma-Okia, W., Bell, J. P., James, R., Vondou, D. A., et al. (2018). Consequences of 1.5°C and 2°C global warming levels for temperature and precipitation changes over Central Africa. *Environmental Research Letters*, *13*(5), 1–12. https://doi.org/10.1088/1748-9326/aab048

Prijith, S. S., Srinivasarao, K., Lima, C. B., Gharai, B., Rao, P. V. N., SeshaSai, M. V. R., & Ramana, M. V. (2021). Effects of land use/land cover alterations on regional meteorology over Northwest India. *Science of the Total Environment*, *765*, 142678. https://doi.org/10.1016/j.scitotenv.2020.142678

Remedio, A. R., Teichmann, C., Buntemeyer, L., Sieck, K., Weber, T., Rechid, D., et al. (2019). Evaluation of new CORDEX simulations using an updated Köppen–Trewartha climate classification. *Atmosphere*, *10*(11), 1–25. https://doi.org/10.3390/atmos10110726

Rothfusz, L. P. (1990). *The heat index equation (or, more than you ever wanted to know about heat index)*. National Oceanic and Atmospheric Administration, National Weather Service, Office of Meteorology, 90-23.

Roy, P. S., Ramachandran, R. M., Paul, O., Thakur, P. K., Ravan, S., Behera, M. D., et al. (2022). Anthropogenic land use and land cover changes – A review on its environmental consequences and climate change. *Journal of the Indian Society of Remote Sensing*, *50*(8), 1615–1640. https://doi.org/10.1007/s12524-022-01569-w

Scovronick, N., Sera, F., Acquaotta, F., Garzena, D., Fratianni, S., Wright, C. Y., & Gasparrini, A. (2018). The association between ambient temperature and mortality in South Africa: A time-series analysis. *Environmental Research*, *161*, 229–235. https://doi.org/10.1016/j.envres.2017.11.001

Steadman, R. G. (1979). The assessment of sultriness. Part I: A temperature-humidity index based on human physiology and clothing science. *Journal of Applied Meteorology and Climatology*, *7*, 861–873. https://doi.org/10.1175/1520-0450(1979)018<0861:taospi>2.0.co;2

Sung, T. I., Wu, P. C., Lung, S. C., Lin, C. Y., Chen, M. J., & Su, H. J. (2013). Relationship between heat index and mortality of 6 major cities in Taiwan. *Science of the Total Environment*, *442*, 275–281. https://doi.org/10.1016/j.scitotenv.2012.09.068

Sylla, M. B., Faye, A., Giorgi, F., Diedhiou, A., & Kunstmann, H. (2018). Projected heat stress under 1.5°C and 2°C global warming scenarios creates unprecedented discomfort for humans in West Africa. *Earth's Future*, *6*(7), 1029–1044. https://doi.org/10.1029/2018EF000873

Taguela, T. N., Vondou, D. A., Moufouma-Okia, W., Fotso-Nguemo, T. C., Pokam, W. M., Tanessong, R. S., et al. (2020). CORDEX multi-RCM hindcast over Central Africa: Evaluation within observational uncertainty. *Journal of Geophysical Research: Atmospheres*, *125*(5), 1–21. https://doi.org/10.1029/2019JD031607

Tamoffo, A. T., Amekudzi, L. K., Weber, T., Vondou, D. A., Yamba, E. I., & Jacob, D. (2022). Mechanisms of rainfall biases in two CORDEX-CORE regional climate models at rainfall peaks over central equatorial Africa. *Journal of Climate*, *35*(2), 639–668. https://doi.org/10.1175/JCLI-D-21-0487.1

Tamoffo, A. T., Moufouma-Okia, W., Dosio, A., James, R., Pokam, W. M., Vondou, D. A., et al. (2019). Process-oriented assessment of RCA4 regional climate model projections over the Congo Basin under 1.5°C and 2°C global warming levels: Influence of regional moisture fluxes. *Climate Dynamics*, *53*(3–4), 1911–1935. https://doi.org/10.1007/s00382-019-04751-y

Taylor, K. E., Stouffer, R. J., & Meehl, G. A. (2012). An overview of CMIP5 and the experiment design. *Bulletin of the American Meteorological Society*, *93*(4), 485–498. https://doi.org/10.1175/BAMS-D-11-00094.1

Teichmann, C., Eggert, B., Elizalde, A., Haensler, A., Jacob, D., Kumar, P., et al. (2013). How does a regional climate model modify the projected climate change signal of the driving GCM: A study over different CORDEX regions using REMO. *Atmosphere*, *4*(2), 214–236. https://doi.org/10.3390/atmos4020214

Teichmann, C., Jacob, D., Remedio, A. R., Remke, T., Buntemeyer, L., Hoffmann, P., et al. (2021). Assessing mean climate change signals in the global CORDEX-CORE ensemble. *Climate Dynamics*, *57*, 1269–1292. https://doi.org/10.1007/s00382-020-05494-x

Vondou, D. A., & Haensler, A. (2017). Evaluation of simulations with the regional climate model REMO over Central Africa and the effect of increased spatial resolution. *International Journal of Climatology*, *37*, 741–760. https://doi.org/10.1002/joc.5035

Weber, T., Bowyer, P., Rechid, D., Pfeifer, S., Raffaele, F., Remedio, A. R., et al. (2020). Analysis of compound climate extremes and exposed population in Africa under two different emission scenarios. *Earth's Future*, *8*(9), 1–19. https://doi.org/10.1029/2019EF001473

Weber, T., Haensler, A., Rechid, D., Pfeifer, S., Eggert, B., & Jacob, D. (2018). Analyzing regional climate change in Africa in a 1.5°, 2°, and 3°C global warming world. *Earth's Future*, *6*(4), 643–655. https://doi.org/10.1002/2017EF000714

Weinberger, K. R., Zanobetti, A., Schwartz, J., & Wellenius, G. A. (2018). Effectiveness of National Weather Service heat alerts in preventing mortality in 20 US cities. *Environment International*, *116*, 30–38. https://doi.org/10.1016/j.envint.2018.03.028

Yengoh, G. T., & Ardö, J. (2020). Climate change and the future heat stress challenges among smallholder farmers in East Africa. *Atmosphere*, *11*(7), 1–29. https://doi.org/10.3390/atmos11070753